

Quantification of the Anterior–Centripetal Movement of the Ciliary Muscle During Accommodation Using Dynamic OCT Imaging

Iulen Cabeza-Gil¹, Marco Ruggeri^{2,3}, and Fabrice Manns^{2,3}

¹ Aragón Institute of Engineering Research (i3A), University of Zaragoza, Zaragoza, Spain

² Ophthalmic Biophysics Center, Bascom Palmer Eye Institute, University of Miami Miller School of Medicine, Miami, FL, USA

³ Department of Biomedical Engineering, University of Miami College of Engineering, Coral Gables, FL, USA

Correspondence: Fabrice Manns, Bascom Palmer Eye Institute, 1638 NW 10th Avenue, Miami, FL 33136, USA. e-mail: fmanns@miami.edu

Received: July 16, 2023

Accepted: November 4, 2024

Published: January 16, 2025

Keywords: presbyopia; lens; mechanism of accommodation

Citation: Cabeza-Gil I, Ruggeri M, Manns F. Quantification of the anterior–centripetal movement of the ciliary muscle during accommodation using dynamic OCT imaging. *Transl Vis Sci Technol.* 2025;14(1):17, <https://doi.org/10.1167/tvst.14.1.17>

Purpose: Although the lens undoubtedly plays a major role in presbyopia, altered lens function could be in part secondary to age-related changes of the ciliary muscle. Ciliary muscle changes with accommodation have been quantified using optical coherence tomography, but so far these studies have been limited to quantifying changes in ciliary muscle thickness, mostly at static accommodative states. Quantifying ciliary muscle thickness changes does not effectively capture the dynamic anterior–centripetal movement of the ciliary muscle during accommodation. To address this issue, we present a method to quantify the movement of the ciliary muscle during accommodation using trans-scleral optical coherence tomography images obtained dynamically.

Methods: An image processing framework including distortion correction, geometric transformation, and Procrustes analysis, was used to quantify the anterior–centripetal movement of the ciliary muscle apex and centroid during accommodation. The method was applied in a preliminary study to quantify ciliary muscle displacement and its relation to lens thickness change with accommodation on two young adults and two prepresbyopes.

Results: The magnitude and the direction relative to the pupil plane of the apex/centroid displacement in response to a two diopters (2D) stimulus were 0.16/0.20 mm at 11.3°/30.5° and 0.26/0.34 mm at 6.6°/33.2° for the young adults and 0.20/0.20 mm at 29.7°/40.6° and 0.24/0.40 mm at 33.0°/31.7° for the prepresbyopes, respectively.

Conclusions: This study demonstrates the feasibility of quantifying dynamic anterior–centripetal movement of the ciliary muscle during accommodation using optical coherence tomography. The method better captures the functional response of the muscle than the quantification of thickness changes.

Translational Relevance: We provide a method that holds potential to better understand the age-related changes of the ciliary muscle on presbyopia.

Introduction

Accommodation is the process of changing the eye's power to allow for clear vision of nearby objects. The ciliary muscle is the engine of the accommodation process. Contraction of the ciliary muscle releases the resting zonular tension, allowing the lens to take a more curved shape and thus, increasing the ocular dioptric power.^{1–6} With age, the ability to accommo-

date decreases, leading to presbyopia, the loss of near visual function starting around age 40. Although the primary cause of presbyopia is the stiffening of the lens,^{4,7,8} altered accommodative function could be in part secondary to extralenticular age-related changes, such as changes in the anatomy and displacement of the ciliary muscle and uveal structures with age.^{9,10}

Imaging the ciliary muscle during accommodation has been a challenge.¹¹ Although magnetic resonance imaging has been used,¹² its static nature and lower

resolution have limited its usefulness. Studies using ultrasound biomicroscopy (UBM) have shown age-related changes.^{13–18} However, the need for direct contact with the eye makes it challenging to image the response under natural accommodative conditions. optical coherence tomography (OCT) offers an alternative imaging method that, unlike UBM, is noncontact, high resolution, and high speed, thus representing a promising alternative for assessing the dynamic accommodative response of the ciliary muscle.^{19–27}

Prior OCT studies have investigated changes in ciliary muscle response during accommodation by measuring thickness changes acquired at static accommodative states.^{19–27} These studies provide the muscle shape at the start and end point of accommodation, but they do not capture the dynamics of the anterior–centripetal movement,²⁸ which is the primary function of the ciliary muscle during accommodation.¹⁵ We previously demonstrated the ability to record the changes in shape of the ciliary muscle dynamically during accommodation using OCT.²¹ Dynamic recordings provide information that cannot be obtained from static data, such as the time constant and velocity of the ciliary muscle response or the relation between ciliary muscle movement and the resulting changes in lens shape in real time during accommodation.²¹ These parameters can provide insight into the dynamics of the accommodative plant, which is central to understanding the neural control and the biomechanics of accommodation.

In the prior static or dynamic OCT studies, changes in the shape of the ciliary muscle were quantified typically using thickness measurements obtained at discrete locations along the ciliary muscle or across its entire profile.^{19–27} Ciliary muscle thickness profiles show the change in shape of the ciliary muscle and can be used to quantify the displacement of the apex, but they do not provide a quantitative measurement of the anterior–centripetal movement of the body of the muscle in the longitudinal direction, which determines the direction of the force of accommodation. Studies of this movement and its changes with age could be key in clarifying the causes of presbyopia and optimizing the design of accommodating intraocular lenses. To better assess ciliary muscle function, Stachs et al.¹⁷ quantified the displacement of the center of gravity of three-dimensional UBM images of the ciliary body acquired before and after pharmacological stimulation of accommodation. In their approach, the ciliary muscle was truncated at the same fixed distance, approximately 3 mm, from the scleral spur in the relaxed and accommodated state. Therefore, the contours in the relaxed and accommodated state have different cross-sections, given the forward displacement of the muscle, and the calculated centroid displacement

does not truly represent the movement of the ciliary muscle.

We propose a method to quantify the anterior–centripetal movement of the ciliary muscle during accommodation using dynamic OCT imaging that addresses this limitation by using Procrustes analysis. The proposed method captures the dynamic response of the ciliary muscle, which is to move forward and inward by quantifying the movement of the ciliary muscle centroid and apex, respectively. We demonstrate the application of the method in a preliminary study on four participants.

Methods

Study Design

Trans-scleral OCT images of the ciliary muscle acquired on the left eye of four human participants, two young and two prepresbyopic, using a system that was described previously^{21,29–31} were collected specifically for this study (Table 1). The study followed a protocol approved by the Institutional Review Board at the University of Miami. All participants consented before enrollment in the study.

Imaging Protocol

The imaging system consisted of two separate spectral domain (SD) OCT systems precisely synchronized and operating at central wavelengths of 1325 nm and 840 nm for acquiring trans-scleral ciliary muscle and anterior segment (AS) images at a frame rate of 26 Hz.²¹ AS images were used to quantify changes in the lens thickness (LT) during accommodation, which was used as an objective measure of the accommodative response. The OCT systems were combined and synchronized with a dual-channel visual fixation target designed to produce step stimuli of accommodation during OCT image acquisition. The two OCT systems are synchronized with an uncertainty of ± 1 frame, or ± 38.6 ms.¹⁹ The ciliary muscle unit is based on a commercially available OCT platform (TELESTO,

Table 1. Data Sample Collected

Participant	Age (Years)	Refractive Error	Accommodation Stimulus (D)
1	22	–2.75	2, 4
2	26	–1.50	2, 4
3	45	+1.75	2
4	45	–4.50	2

Prepresbyopic participants were only subjected to 2 D of accommodation stimulus owing to presbyopic limitations.

Thorlabs Inc., Newton, NJ) that produces images with an axial resolution of 7.5 μm (in air) over an axial range of 2.5mm (in air). The AS system features an axial resolution of approximately 8 μm (in air) over a range of 13.5 mm.

Each recording consisted of a sequence of 160 ciliary muscle OCT and 80 AS OCT images acquired during the response to a step stimulus of accommodation. The ciliary muscle–OCT unit operated at 28,000 A-lines/s with 897 lines per frame (512×897 pixels) and the AS-OCT was operated at 12,500 A-lines with 400 lines per frame (400×2048 pixels). The amplitude of the accommodation step stimulus was two-diopters (2D) for the presbyopic participants, and 2D and four-diopters (4D) for the young participants (Table 1). Each recording lasted 6.17 seconds; the accommodation step stimulus was triggered 1.54 seconds after the start of an acquisition.

Quantification of the Anterior–Centripetal Movement Ciliary Muscle

Figure 1 outlines the procedure for quantifying the anterior–centripetal movement of the ciliary muscle during accommodation. The process involves several steps:

- 1) Correction of any misalignment (eye movement) during dynamic recording and enhancement of ciliary muscle contrast in OCT images using processing methods;
- 2) Segmentation of the ciliary muscle shape, scleral and anterior iris boundaries and correction of the segmented parts for refractive distortion; and
- 3) Rotation of the corrected ciliary muscle shape and sclera according to the iris, which serves as the reference plane in the image;
- 4) Quantification of the displacement of the ciliary muscle's apex and centroid using Procrustes analysis.

Processing of the Raw Trans-scleral OCT Images

The ciliary muscle images of each recording are processed to correct for eye movements using the 'imregister' MATLAB function. To enhance contrast, each pair of consecutive images were averaged, resulting in a sequence of 80 images for each recording. The overall contrast of the averaged images was further improved with the 'imadjust' MATLAB function, which is based on the following function:

$$y = \left(\frac{x - a}{b - a} \right)^\gamma, \quad (1)$$

where y and x are the resulting and original pixel values, respectively, γ specifies the distribution of the image histogram (i.e., the brightness of the image), and a and b determine the lower and upper limits calculated for contrast stretching of the image, respectively. Parameters a and b were calculated automatically through the 'stretchlim' MATLAB function, and $\gamma = 1.5$ was applied to all images.

Segmentation and Distortion Correction of the OCT Images

The preprocessed trans-scleral images are segmented with a custom-developed automatic tool based on fully convolutional neural networks³² (Fig. 1). The anterior iris was manually segmented only for the first image of the recording. We then implemented an algorithm to correct image distortion owing to the refraction of the OCT beam at the air–sclera, sclera–ciliary muscle, and sclera–anterior humor boundaries based on the vector form of Snell's law.²⁹ For distortion correction, we used the group refractive indices of the sclera (1.415) and ciliary muscle (1.380) estimated at 1325 nm.²¹ The anterior conjunctiva was included in the scleral segmentation.

Selection of the Reference System

The peripheral portion of the anterior surface of the iris was used as a reference plane for the registration and alignment of the images. Specifically, all images were initially registered according to the first image, and then rotated to align the iris along the x axis of the coordinate system, assuming that the position of the iris does not change significantly axially during the accommodative response. The constriction of the iris or the radial movement does not affect this assumption. This allowed for precise comparison and measurement of the anterior–centripetal movement of the ciliary muscle.

The outer scleral boundary of all segmentations was then re-aligned using the iterative closest point method³³ assuming that the outer scleral boundary remains approximately constant during accommodation³⁴ to reduce fluctuations in the quantification of ciliary muscle displacement caused by small eye movements. This additional step minimized potential misalignment errors resulting from the registration process, further enhancing the accuracy of the analysis.

Quantification of the Ciliary Muscle Apex and Centroid

We measured the anterior–centripetal movement of the ciliary muscle by measuring the displacement of the ciliary muscle centroid and apex, respectively (Fig. 1). The apex was defined as the point with the maximum ciliary muscle thickness (i.e., maximum distance from

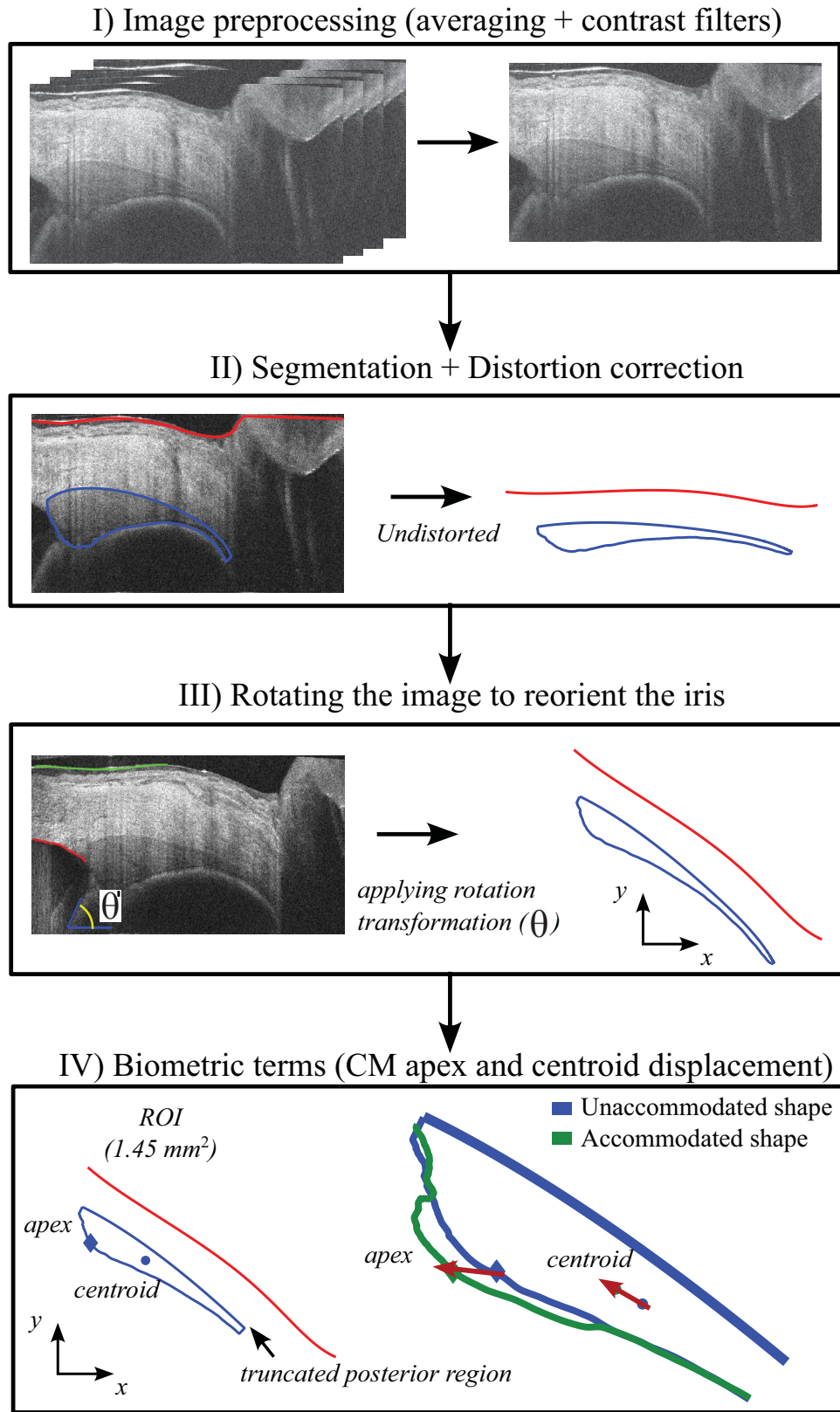


Figure 1. Method to quantify the displacement of the apex and centroid of the ciliary muscle. (I) Image processing to correct for eye movement and improve image contrast. (II) Segmentation and distortion correction of the ciliary muscle and the sclera. (III) The ciliary muscle and sclera are rotated to align the iris in the same direction as in the AS image, that is, ensuring that it is aligned at 0° with respect to the lens. (IV) biometry of the ciliary muscle obtained through a statistical shape method (Procrustes analysis).

posterior scleral boundary) in the unaccommodated state. To track the apex during the corresponding frames, we performed a Procrustes analysis³⁵ with the assumption that the ciliary muscle's volume remains constant during accommodation. Procrustes analysis enables a comparison of the deformed and undeformed ciliary muscle shape in successive frames, including translation and rotation, enabling us to track the movement of the ciliary muscle apex or centroid. The initial position of the apex is defined as the point of maximum thickness of the unaccommodated state. As the position of this point shifts and the ciliary muscle deforms during accommodation, in subsequent images, the displaced apex may no longer correspond to the point of maximum thickness.

The Procrustes analysis assumes a constant volume of the ciliary muscle. It therefore requires that the same area of the ciliary muscle is segmented across each dataset. We then chose a specific region of interest of 1.45 mm² that captures most of the muscle's cross-section while excluding the distal end (Fig. 1). This approximation covers more than 85% of the area of the ciliary muscles analyzed in the study, with a length of more than 4.0 mm from the scleral spur. The centroid was then calculated as a measure of the average of the contour for each OCT frame as follows:

$$C(x, y) = \frac{p_1 + p_2 + \dots + p_n}{n}, \quad (2)$$

where n (500) is the total number of equally spaced perimetral points, $p(x,y)$, representing the ciliary muscle shape (Fig. 1, blue contour).

Changes in the apex and centroid of the ciliary muscle are calculated as the magnitude of the displacement. For comparative purposes, the changes in ciliary muscle thickness were also calculated by measuring the distance of the scleral–muscle border and the muscle–pigmented epithelium border along the direction perpendicular to the scleroconjunctival–air interface.³⁶

Quantification of LT

A custom automated segmentation algorithm was applied to each of the 80 OCT images of the AS to detect the anterior and posterior boundaries of the lens along the A-line passing through the pupil center and calculating the central thickness.²¹ The measured optical thickness was converted into a geometrical LT assuming an average refractive index of 1.408 for the lens in the age range of the participants included in the study.³⁷

All biometrical changes (ciliary muscle apex, ciliary muscle centroid, and LT) for each accommodative

stimulus were then calculated as the difference between the average values calculated from the start of the acquisition to the stimulus onset (first 1.54 seconds; participant unaccommodated), and at the end of the recording (last 1.67 seconds; participant fully accommodated).

Results

A representative sample of the anterior–centripetal movement of the ciliary muscle and thickness during accommodation acquired from participant 4 is presented (Figs. 2 and 3). The results for the remaining participants and a video showing the dynamic displacement of the ciliary muscle are reported in the Supplemental Materials.

Figure 2A shows the ciliary muscle thickness profile for participant 4 in the accommodated and unaccommodated state for a 2D accommodation stimulus. Figure 2B shows the temporal change in ciliary muscle thickness at the point of maximum thickness and at 3 mm from the scleral spur. For participant 4, the changes in maximum thickness of the ciliary muscle and ciliary muscle 3 mm from the scleral spur were 0.10 ± 0.01 mm and -0.02 ± 0.01 mm, respectively.

Figure 2C shows the time dependence of the displacement of the apex and centroid of the ciliary muscle and the change in LT for a 2D accommodation stimulus. LT for participant 4 increased by 0.08 ± 0.004 mm, the ciliary muscle apex displacement was 0.24 ± 0.02 mm, and the ciliary muscle centroid displacement was 0.40 ± 0.03 mm. Figure 2D shows the change in LT vs. ciliary muscle movement. The results show that there is a displacement of the ciliary muscle before the lens shape starts to change, that is, 0.09 ± 0.04 mm and 0.19 ± 0.05 mm for the ciliary muscle apex and centroid, respectively. This difference was calculated as the average of the four ciliary muscle displacement values recorded just before the change in LT reached a threshold set slightly above the axial resolution of the AS-OCT system (0.01 mm).

Figure 3 shows the 2D displacement of the apex and centroid of the ciliary muscle during the 2D accommodative stimulus in participant 4 quantified considering a horizontal iris. The X- and Y- components of the displacement were -0.20 ± 0.02 mm and 0.13 ± 0.02 mm, respectively, for the apex and -0.34 ± 0.03 mm and 0.21 ± 0.02 mm, respectively, for the centroid, where the values represent the mean \pm standard deviation. The X component represents the centripetal movement toward the lens (along the plane of the iris). The measurement of the apex is noisier than

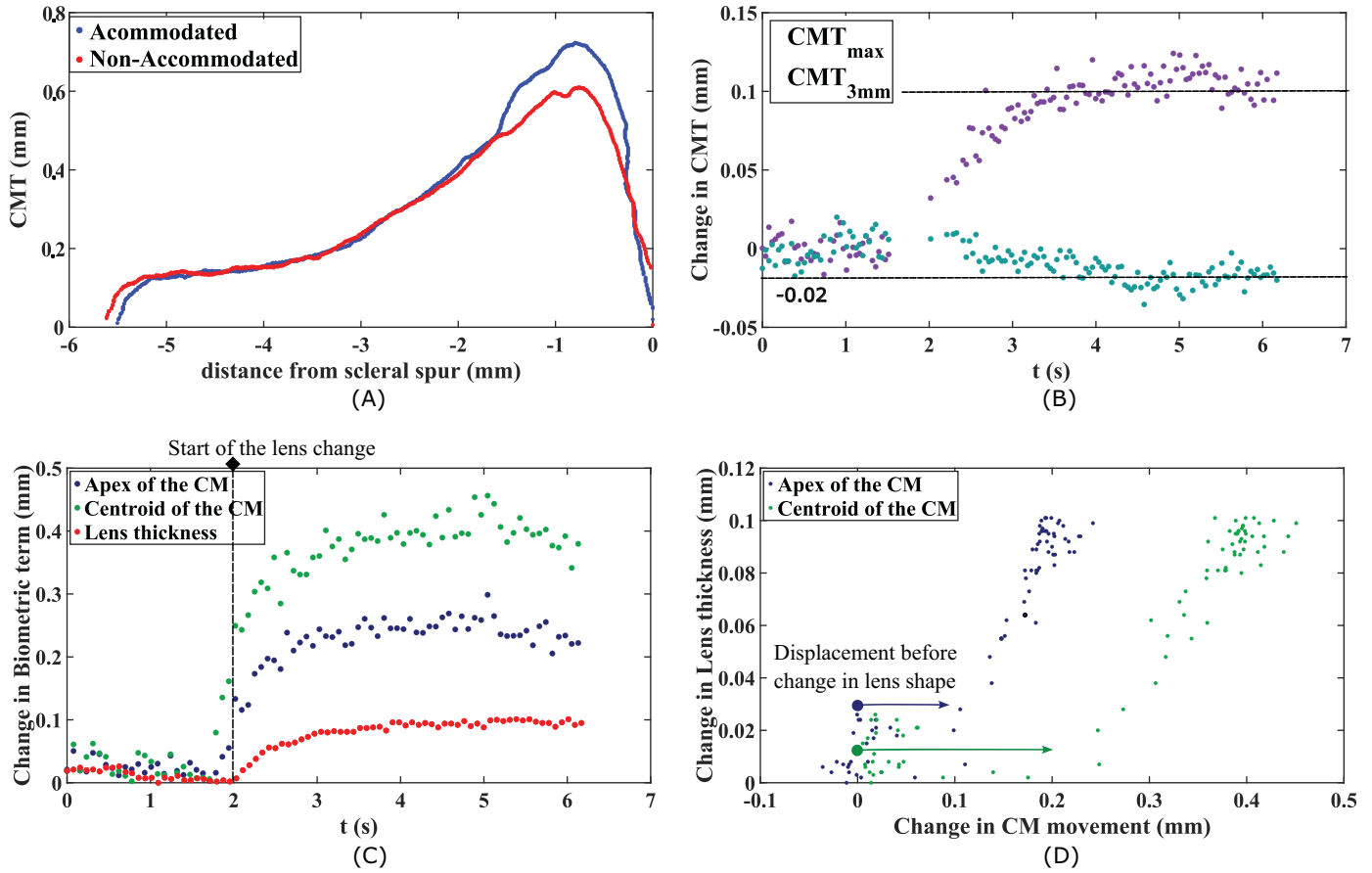


Figure 2. (A) Ciliary muscle thickness profile in the unaccommodated and accommodated state for a 2D accommodation stimulus in participant 4. (B) Change in the ciliary muscle thickness at the point of maximum thickness (CMT_{max}) and at 3 mm (CMT_{3mm}) from the scleral spur. There is an increase of 0.10 mm of CMT_{max} and a decrease of -0.02 mm of CMT_{3mm} . (C) Change of the ciliary muscle apex (navy) and centroid (blue), together with the change in LT (red), according to time for a 2D accommodative stimulus for participant 4. The accommodation stimulus was triggered at 1.54 s. (D) Change in apex and centroid against the change in LT.

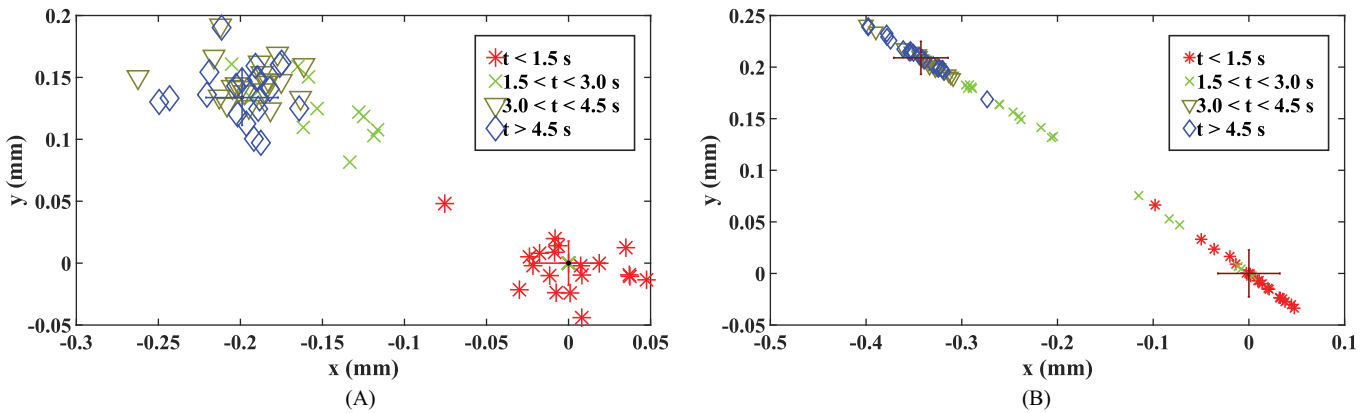


Figure 3. Two-dimensional displacement of the apex (A) and centroid (B) of the ciliary muscle for a 2D accommodation stimulus for participant 4. The stimulus was applied at $t = 1.54$ seconds.

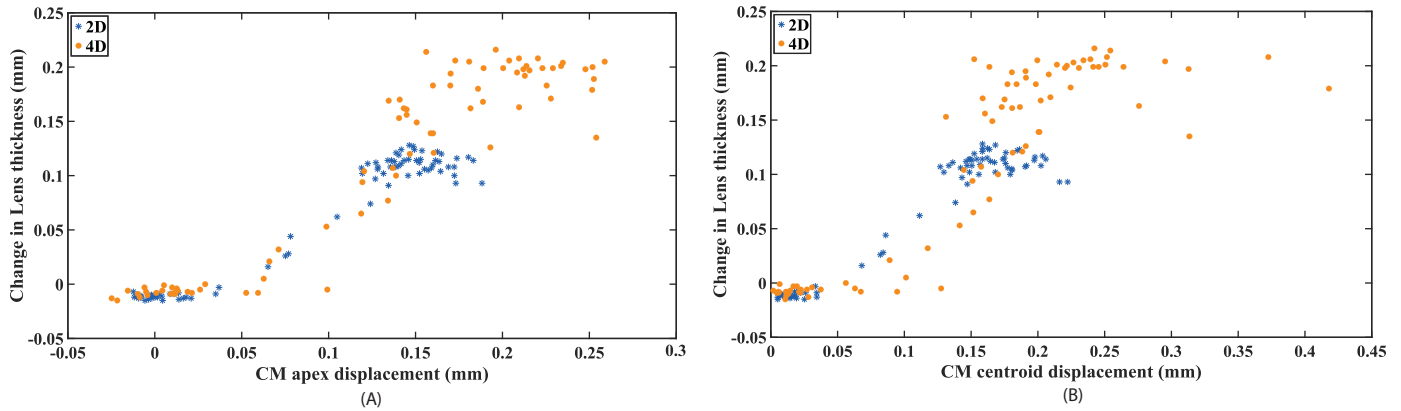


Figure 4. Change in LT according to ciliary muscle apex (A) and centroid (B) displacement for 2D and 4D accommodation stimuli.

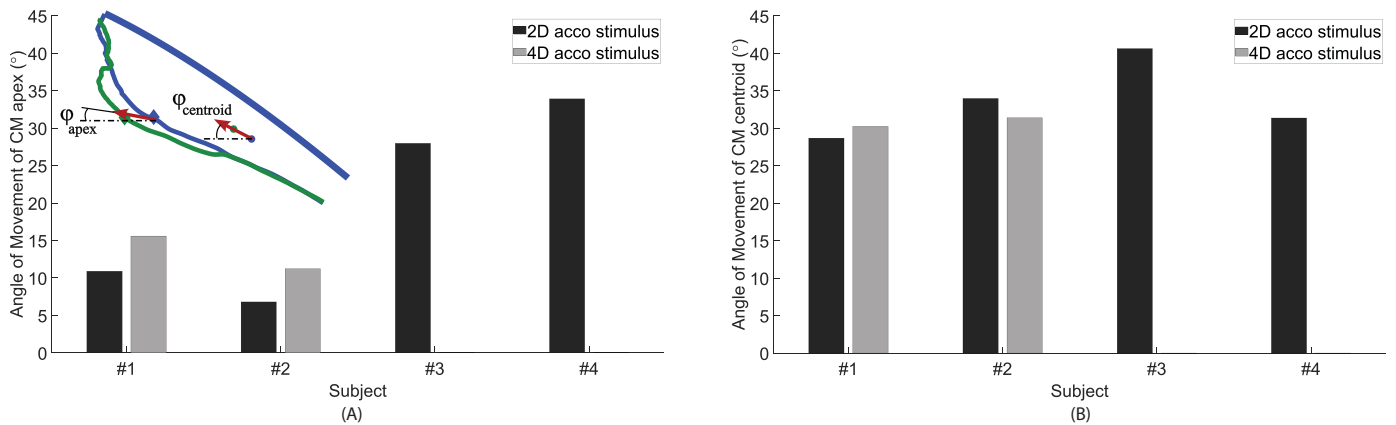


Figure 5. Ciliary muscle apex (A) and centroid (B) angle of movement. Participants 1 and 2 are young participants. Participants 3 and 4 are prepresbyopic participants.

the centroid owing to higher uncertainty in the segmentation in the region of the apex. The centroid displacement shows that the anterior movement follows a nearly linear path aligned with the longitudinal fibers of the ciliary muscle during accommodation.

For the 2D stimulus, the mean and standard deviation of the ciliary muscle displacement were 0.21 ± 0.07 mm and 0.20 ± 0.06 mm for the apex and 0.27 ± 0.10 mm and 0.30 ± 0.14 mm for the centroid, for the young and prepresbyopic participants, respectively. In the young group, for the 4D stimulus, the ciliary muscle apex and centroid displacements were 0.23 ± 0.08 mm and 0.27 ± 0.07 mm, respectively.

To illustrate the distinction between 2D and 4D accommodation stimuli, we present in Figures 4A and B the variations in LT with respect to the displacement of the ciliary muscle apex and centroid for participant 1. When subjected to a 2D accommodation stimulus,

the LT changed by 0.11 ± 0.01 mm, and the ciliary muscle apex and centroid displacement were 0.16 ± 0.01 mm and 0.20 ± 0.02 mm, respectively. In contrast, under a 4D accommodation stimulus, the LT changed by 0.20 ± 0.01 mm, with the ciliary muscle apex and centroid displacement measuring 0.17 ± 0.02 mm and 0.22 ± 0.02 mm, respectively.

Figure 5 shows the angle of the anterior–centripetal movement of the ciliary muscle, which quantifies the direction of the ciliary muscle movement. The angle was calculated as the arc tangent between the Y and X component displacement of the ciliary muscle apex and centroid (Table 2). The angles of movement of the ciliary muscle apex and centroid had an average value of 11.12° and 30.06° for the young participants (4D stimulus) and 30.93° and 36.15° for the prepresbyopic participants, respectively. Table 2 lists the changes in ciliary muscle movement for all participants and accommodation stimuli.

Table 2. Main Biometric Terms of the Recordings: the X and Y Components of the Ciliary Muscle (CM) Apex and Centroid Displacement, Together with the Corresponding Displacement Magnitude, the Ciliary Muscle Thickness, and the LT Change

Participant	Demand	CM Apex			CM Centroid			CM Thickness			LT Change (mm)
		X Component (mm)	Y Component (mm)	Magnitude (mm)	X Component (mm)	Y Component (mm)	Magnitude (mm)	Maximum CMT (mm)	CMT at 3 mm (mm)		
		1	2D	-0.15 ± 0.01	0.03 ± 0.01	0.16 ± 0.01	-0.17 ± 0.02	0.10 ± 0.01	0.20 ± 0.02	0.047 ± 0.007	
1	4D	-0.21 ± 0.05	0.05 ± 0.03	0.17 ± 0.02	-0.23 ± 0.05	0.13 ± 0.03	0.22 ± 0.02	0.051 ± 0.006	-0.021 ± 0.008	0.20 ± 0.01	
2	2D	-0.26 ± 0.07	0.03 ± 0.03	0.26 ± 0.06	-0.29 ± 0.09	0.19 ± 0.06	0.34 ± 0.09	0.047 ± 0.013	-0.003 ± 0.007	0.08 ± 0.01	
2	4D	-0.28 ± 0.04	0.05 ± 0.02	0.29 ± 0.04	-0.27 ± 0.06	0.16 ± 0.03	0.32 ± 0.04	0.052 ± 0.012	0.15 ± 0.01	0.15 ± 0.01	
3	2D	-0.14 ± 0.04	0.08 ± 0.03	0.20 ± 0.02	-0.14 ± 0.06	0.12 ± 0.05	0.20 ± 0.08	0.055 ± 0.013	-0.007 ± 0.015	0.08 ± 0.01	
4	2D	-0.20 ± 0.02	0.13 ± 0.02	0.24 ± 0.02	-0.34 ± 0.02	0.21 ± 0.02	0.40 ± 0.02	0.104 ± 0.009	-0.018 ± 0.007	0.08 ± 0.01	

Discussion

This study presents a method for quantifying the anterior–centripetal movement of the ciliary muscle during accommodation using dynamic OCT imaging based on Procrustes analysis. The method was demonstrated in a preliminary study on 4 participants. The dynamic analysis allows us to quantify the displacement of the body of the ciliary muscle and its relationship with the change in LT during accommodation. The analysis provides parameters such as the amplitude, direction, time constant, and velocity of the ciliary muscle movement, which are relevant in studies of the biomechanics and neural control of accommodation.^{5,6}

A larger sample size is required to gain information regarding the response of the ciliary muscle during accommodation and its relation to changes in lens shape. However, our preliminary study helps to demonstrate the knowledge that can be gained using this method and its potential applications in the study of accommodation dynamics. For instance, our preliminary results show that the method allows us to quantify differences in the amplitude and orientation of the ciliary muscle movement and quantify their impact on the amplitude and dynamics of the changes in lens shape. These differences could influence the forces applied to the lens. Further studies utilizing this method on a larger sample size could therefore help determine if there are age-related changes in these parameters that could be a factor in presbyopia.

Previous OCT studies typically quantified the changes in ciliary muscle with accommodation by using thickness measurements at discrete positions, or the thickness profile.^{19–27} Quantifying the ciliary muscle thickness can offer valuable insight into the overall change in shape of the muscle or changes at discrete positions, such as the forward and inward movement of the apex.^{19,20,26,29} However, thickness measurements do not capture the overall net movement of the body of the ciliary muscle during accommodation quantitatively, which determines the direction of the force of accommodation²⁸ that releases the resting zonular tension and pulls the choroid forward (the anterior–centripetal movement of the ciliary muscle). This movement of the entire muscle is clearly visible in dynamic UBM images,^{10,13,15} and we have previously shown that it can also be visualized using dynamic OCT imaging.²¹ Our study demonstrates the feasibility of quantifying this movement from dynamic OCT recordings by measuring the displacement of the apex or centroid of the ciliary muscle contour using Procrustes analysis. The centroid displacement repre-

sents a measurement of displacement of the more posterior longitudinal fibers of the ciliary muscle that cannot be captured using thickness measurements. The apex displacement produced using our method is different from the apex displacement predicted from thickness measurements. The Procrustes analysis calculates the displacement of contour points from the deformation of the contour, whereas methods based on thickness define the apex as the point of maximum thickness measured in the transverse direction.³⁶ In our study, we find that the magnitude of the apex displacement produced using the Procrustes analysis (≤ 0.13 mm/D) is much more pronounced than the changes in apex thickness (≤ 0.05 mm/D).¹⁹ We, therefore, expect that the ciliary muscle displacement will provide greater sensitivity in quantifying changes with accommodation or age than thickness measurements.

Overall, the results of our preliminary study are consistent with findings from prior studies using OCT and with the Helmholtz theory of accommodation. As in prior OCT studies, we find an increase in thickness in the anterior region of the ciliary muscle close to the apex and a thinning in the posterior region at 3 mm from the scleral spur.^{19,20,26,29} Our change in thickness profile (Fig. 2B) is also comparable with the findings of Wagner et al.¹⁹ (their Figure 7). Our thickness changes at maximum thickness (0.01 up to 0.05 mm/D) are within the range of previously published studies, which found values of 0.01 up to 0.03 mm/D.^{19,20,26,29} In addition, as in our prior study,²¹ we find that there is a lag between the response of the muscle and the lens, which is more pronounced in older adults. No obvious lag between the movement of the lens and ciliary processes was observed in gonioscopic video recordings acquired in nonhuman primates during accommodation induced by stimulation of the Edinger-Westphal nucleus stimulated using implanted electrodes. However, this difference could be due to differences in methodology (stimulated response in iridectomized monkeys vs. natural response in human participants). Further studies on a larger population sample are required to confirm the presence of the lag and its age dependence.

In the same age range, the centroid displacements found by Stachs et al.¹⁷ using UBM (0.04 to 0.26 mm) are lower than our results (0.20 to 0.40 mm), even though their study relied on pharmacological stimulation, which is expected to produce more pronounced changes. The reason for these differences is most likely that Stachs et al.¹⁷ truncated the ciliary muscle more anterior, at approximately 3 mm from the scleral spur, that they truncated the ciliary muscle at the same fixed distance from the scleral spur in the relaxed and accommodated states, and that they included the ciliary

processes in their contour. In a separate analysis, we found that the magnitude of the centroid displacement decreases by approximately 25% if the OCT images are truncated at 3 mm. The effect of truncation is discussed further elsewhere in this article.

The proposed OCT-based method offers several biometric parameters that could be used to better understand the age-related changes in the ciliary muscle, such as, for example, the displacement of the ciliary muscle apex and centroid. We believe that the most suitable metric will depend on the research question being addressed. It seems the centroid movement might be driven more by the longitudinal fibers, whereas the ciliary muscle apex might be driven more by radial and circular fibers. Apex displacement is more directly related to the interaction with the lens, because the displacement of the apex more directly determines the tension on the zonules. We expect that the combination of multiple metrics will help to better understand the muscle response as a whole. For instance, comparing the centroid displacement with the apex displacement and studying age-related changes could help understand if the ciliary muscle displacement remains constant with age, but apex movement changes, or the age-related changes, are the same.

The proposed method was developed using the iris as a reference plane and Procrustes analysis to relate the shape of the ciliary muscle across different time points during the accommodative process, providing a new approach to measure the anterior–centripetal movement of the ciliary muscle during accommodation in dynamic OCT imaging.

For this preliminary study, we somewhat arbitrarily chose a fixed area of 1.45 mm² for the Procrustes analysis, because we found that it captured most of the ciliary muscle in the study participants (>85% of the area and >4.0 mm from the scleral spur), except for the distal end. The position of the centroid may be shifted if instead we would have included the entire ciliary muscle all the way to the posterior insertion zonule. In addition, the calculated centroid displacement will be affected by interindividual variations in the shape of the muscle or the size of the truncated area. For instance, with a fixed truncated area, we expect that we will find a smaller overall displacement with a more pronounced inward component for a shorter muscle relative to a longer muscle. However, in a separate analysis, we found that these effects can be largely compensated for by expressing the displacement in percent of the initial length. Further analyses on a larger sample will help to quantify the effect of interindividual variations and determine the optimal approach to quantify displacement (e.g., relative vs. absolute, size of the area).

Acquiring dynamic images of the ciliary muscle during accommodation has also the advantage of ensuring that the same region of the ciliary muscle is imaged at different accommodative states during the same imaging session, whereas imaging of the ciliary muscle at static accommodative states may introduce misalignment errors owing to the need of acquiring images in different sessions.²¹ In our method, the greatest source of error is the variability of the segmentation at the ciliary muscle's apex owing to the lower OCT image contrast in this region.^{30,32} Our previous studies show that the variability of ciliary muscle thickness measurement in the region of the apex is on the order of $\pm 45 \mu\text{m}$. This is a known limitation that could be addressed by increasing the signal to noise ratio of the images, for instance by using a high incident power.³¹ The maximum power of the research-grade commercial spectral domain OCT system used in the present study was 4 mW, well below the exposure limit at 1300 nm. In the two participants (1 and 4) where the images of the ciliary muscle apex had high quality, the variability of the measurements was minimal.

Acknowledgments

I. Cabeza-Gil thanks NextGenerationEU (Margarita Salas) for research support.

Supported by National Eye Institute Grants R01EY014225, P30EY14801 (Center Core Grant); the Florida Lions Eye Bank and Beauty of Sight Foundation; the Henri and Flore Lesieur Foundation (JMP); and Harry W. Flynn Jr, MD.

Disclosure: **I. Cabeza-Gil**, None; **M. Ruggeri**, None; **F. Manns**, None

References

- de Castro A, Birkenfeld J, Maceo B, et al. Influence of shape and gradient refractive index in the accommodative changes of spherical aberration in nonhuman primate crystalline lenses. *Invest Ophthalmol Vis Sci*. 2013;54(9):6197–6207.
- Martinez-Enriquez E, Pérez-Merino P, Velasco-Ocana M, Marcos S. OCT-based full crystalline lens shape change during accommodation in vivo. *Biomed Opt Express*. 2017;8(2):918–933.
- Ramasubramanian V, Glasser A. Objective measurement of accommodative biometric changes using ultrasound biomicroscopy. *J Cataract Refract Surg*. 2015;41(3):511–526.
- Cabeza-Gil I, Grasa J, Calvo B. A validated finite element model to reproduce Helmholtz's theory of accommodation: a powerful tool to investigate presbyopia. *Ophthalm Physiol Opt*. 2021;41(6):1241–1253.
- Croft MA, Glasser A, Kaufman PL. Accommodation and presbyopia. *Int Ophthalmol Clin*. 2001;41(2):33–46.
- Glasser A, Kaufman PL. The mechanism of accommodation in primates. *Ophthalmology*. 1999;106(5):863–872.
- Weeber HA, Eckert G, Pechhold W, van der Heijde RGL. Stiffness gradient in the crystalline lens. *Graefes Arch Clin Exp Ophthalmol*. 2007;245(9):1357–1366.
- Cabeza-Gil I, Grasa J, Calvo B. A numerical investigation of changes in lens shape during accommodation. *Sci Rep*. 2021;11(1):9639.
- Croft MA, Kaufman PL. Accommodation and presbyopia: the ciliary neuromuscular view. *Ophthalmol Clin North Am*. 2006;19(1):13–24.
- Croft MA, Nork TM, Heatley G, McDonald JP, Katz A, Kaufman PL. Intraocular accommodative movements in monkeys; relationship to presbyopia. *Exp Eye Res*. 2022;222:109029.
- Fernández-Vigo JI, Kudsieh B, Shi H, De-Pablo-Gómez-de-Liaño L, Fernández-Vigo JA, García-Feijóo J. Diagnostic imaging of the ciliary body: technologies, outcomes, and future perspectives. *Eur J Ophthalmol*. 2022;32(1):75–88.
- Strenk SA, Semmlow JL, Strenk LM, Munoz P, Gronlund-Jacob J, DeMarco JK. Age-related changes in human ciliary muscle and lens: a magnetic resonance imaging study. *Invest Ophthalmol Vis Sci*. 1999;40(6):1162–1169.
- Croft MA, McDonald JP, Katz A, Lin TL, Lütjen-Drecoll E, Kaufman PL. Extralenticular and lenticular aspects of accommodation and presbyopia in human versus monkey eyes. *Invest Ophthalmol Vis Sci*. 2013;54(7):5035–5048.
- Croft MA, Lütjen-Drecoll E, Kaufman PL. Age-related posterior ciliary muscle restriction – a link between trabecular meshwork and optic nerve head pathophysiology. *Exp Eye Res*. 2017;158:187–189.
- Croft MA, McDonald JP, Nadkarni Nv, Lin TL, Kaufman PL. Age-related changes in centripetal ciliary body movement relative to centripetal lens movement in monkeys. *Exp Eye Res*. 2009;89(6):824–832.
- Jeon S, Lee WK, Lee K, Moon NJ. Diminished ciliary muscle movement on accommodation in myopia. *Exp Eye Res*. 2012;105:9–14.

17. Stachs O, Martin H, Kirchhoff A, Stave J, Terwee T, Guthoff R. Monitoring accommodative ciliary muscle function using three-dimensional ultrasound. *Graefes Arch Clin Exp Ophthalmol*. 2002;240(11):906–912.
18. Croft MA, Nork MT, McDonald JP, Katz A, Lütjen-Drecoll E, Kaufman PL. Accommodative movements of the vitreous membrane, choroid, and sclera in young and presbyopic human and nonhuman primate eyes. *Invest Ophthalmol Vis Sci*. 2013;54(7):5049–5058.
19. Wagner S, Zrenner E, Strasser T. Ciliary muscle thickness profiles derived from optical coherence tomography images. *Biomed Opt Express*. 2018;9(10):5100–5114.
20. Lossing LA, Sinnott LT, Kao CY, Richdale K, Bailey MD. Measuring changes in ciliary muscle thickness with accommodation in young adults. *Optom Vis Sci*. 2012;89(5):719–726.
21. Ruggeri M, de Freitas C, Williams S, et al. Quantification of the ciliary muscle and crystalline lens interaction during accommodation with synchronous OCT imaging. *Biomed Opt Express*. 2016;7(4):1351–1364.
22. Kaphle D, Schmid KL, Davies LN, Suheimat M, Atchison DA. Ciliary muscle dimension changes with accommodation vary in myopia and emmetropia. *Invest Ophthalmol Vis Sci*. 2022;63(6):24.
23. Sheppard AL, Davies LN. In vivo analysis of ciliary muscle morphologic changes with accommodation and axial ametropia. *Invest Ophthalmol Vis Sci*. 2010;51(12):6882.
24. Owusu E, Shasteen NM, Mitchell GL, et al. Impact of accommodative insufficiency and accommodative/vergence therapy on ciliary muscle thickness in the eye. *Ophthalm Physiol Opt*. 2023;43(5):947–953.
25. Richdale K, Sinnott LT, Bullimore MA, et al. Quantification of age-related and per diopter accommodative changes of the lens and ciliary muscle in the emmetropic human eye. *Invest Ophthalmol Vis Sci*. 2013;54(2):1095–1105.
26. Esteve-Taboada JJ, Domínguez-Vicent A, Monsálvez-Romín D, Del Águila-Carrasco AJ, Montés-Micó R. Non-invasive measurements of the dynamic changes in the ciliary muscle, crystalline lens morphology, and anterior chamber during accommodation with a high-resolution OCT. *Graefes Arch Clin Exp Ophthalmol*. 2017;255(7):1385–1394.
27. Kaphle D, Schmid KL, Davies LN, Suheimat M, Atchison DA. Ciliary muscle dimension changes with accommodation vary in myopia and emmetropia. *Invest Ophthalmol Vis Sci*. 2022;63(6):24.
28. Bailey MD. How should we measure the ciliary muscle? *Invest Ophthalmol Vis Sci*. 2011;52(3):1817–1818.
29. Ruggeri M, Hernandez V, de Freitas C, Manns F, Parel J-M. Biometry of the ciliary muscle during dynamic accommodation assessed with OCT. San Francisco: *Ophthalmic Technologies XXIV*. 2014;8930.
30. Chang Y-C, Liu K, Cabot F, et al. Variability of manual ciliary muscle segmentation in optical coherence tomography images. *Biomed Opt Express*. 2018;9(2):791–800.
31. Mesquita GM, Patel D, Chang Y-C, et al. In vivo measurement of the attenuation coefficient of the sclera and ciliary muscle. *Biomed Opt Express*. 2021;12(8):5089–5106.
32. Cabeza-Gil I, Ruggeri M, Chang Y-C, Calvo B, Manns F. Automated segmentation of the ciliary muscle in OCT images using fully convolutional networks. *Biomed Opt Express*. 2022;13(5):2810–2823.
33. Bergström P, Edlund O. Robust registration of surfaces using a refined iterative closest point algorithm with a trust region approach. *Numerical Algorithms*. 2017;74(3):755–799.
34. Cabeza-Gil I, Manns F, Calvo B, Ruggeri M. Quantification of scleral changes during dynamic accommodation. *Exp Eye Res*. 2023;230:109441.
35. Dai M, Kurtek S, Klassen E, Srivastava A. Statistical shape analysis. In: *Computer Vision*. Cham: Springer; 2020, https://doi.org/10.1007/978-3-030-03243-2_778-1.
36. Straßer T, Wagner S, Zrenner E. Review of the application of the open-source software CilOCT for semi-automatic segmentation and analysis of the ciliary muscle in OCT images. *PLoS One*. 2020;15(6):e0234330.
37. Uhlhorn SR, Borja D, Manns F, Parel J-M. Refractive index measurement of the isolated crystalline lens using optical coherence tomography. *Vision Res*. 2008;48(27):2732–2738.